

Validating quantum-supremacy experiments with exact and fast tensor network contraction

Yong Liu,^{1,*} Yaojian Chen,^{2,*} Chu Guo,^{3,†} Jiawei Song,⁴ Xinmin Shi,⁵ Lin Gan,^{2,4,‡} Wenzhao Wu,⁴ Wei Wu,⁴ Haohuan Fu,^{2,4,§} Xin Liu,^{1,4,¶} Dexun Chen,⁴ Guangwen Yang,^{1,2,4} and Jiangang Gao⁶

¹Zhejiang Lab, Hangzhou, 311121, China

²Tsinghua University, Beijing, 100084, China

³Key Laboratory of Low-Dimensional Quantum Structures and Quantum Control of Ministry of Education, Department of Physics and Synergetic Innovation Center for Quantum Effects and Applications, Hunan Normal University, Changsha 410081, China

⁴National Supercomputing Center in Wuxi, Wuxi, 214000, China

⁵Information Engineering University, Zhengzhou, 450001, China

⁶National Research Center of Parallel Computer Engineering and Technology, Beijing 100190, China

(Dated: December 12, 2022)

The quantum circuits that declare quantum supremacy, such as Google Sycamore [Nature **574**, 505 (2019)], raises a paradox in building reliable result references. While simulation on traditional computers seems the sole way to provide reliable verification, the required run time is doomed with an exponentially-increasing compute complexity. To find a way to validate current “quantum-supremacy” circuits with more than 50 qubits, we propose a simulation method that exploits the “classical advantage” (the inherent “store-and-compute” operation mode of von Neumann machines) of current supercomputers, and computes uncorrelated amplitudes of a random quantum circuit with an optimal reuse of the intermediate results and a minimal memory overhead throughout the process. Such a reuse strategy reduces the original linear scaling of the total compute cost against the number of amplitudes to a sublinear pattern, with greater reduction for more amplitudes. Based on a well-optimized implementation of this method on a new-generation Sunway supercomputer, we directly verify Sycamore by computing three million exact amplitudes for the experimentally generated bitstrings, obtaining an XEB fidelity of 0.191% which closely matches the estimated value of 0.224%. Our computation scales up to 41,932,800 cores with a sustained single-precision performance of 84.8 Pflops, which is accomplished within 8.5 days. Our method has a far-reaching impact in solving quantum many-body problems, statistical problems as well as combinatorial optimization problems where one often needs to contract many tensor networks which share a significant portion of tensors in common.

I. INTRODUCTION

Ever since initially visioned by Feynman in 1982 [1], quantum computing has experienced 40 years of theoretical and experimental developments [2–9], starting to demonstrate a quantum advantage over classical computers in the era of noisy intermediate scale quantum computing [10]. A major experimental milestone is the *quantum supremacy* experiment conducted with the Google Sycamore 53-qubit superconducting quantum processor in 2019 [11], which demonstrates 10^9 times better capability for sampling a random quantum circuit (RQC) over the fastest classical supercomputer Summit at that time. The more recent 56-qubit and 60-qubit Zuchongzhi quantum processors are estimated to be around 26 and 40,000 times harder than Sycamore to classically simulate [12, 13].

In the RQC sampling task, one runs a RQC on a (noisy) quantum processor and then measures it to produce a number of bitstrings (samples). While generating a number of samples is an easy task for quantum processors, simulating this task on a classical computer is a hard problem [14–17], even for noisy RQCs [18, 19] (noticing a recent work which proposed a polynomial but impractical algorithm for simulating

constant-noise RQCs [20]). The enormous difficulty of simulating more than 50 qubits on classical computers brings us a paradox in building reliable verification results. With classical simulations being the sole way to verify the noisy RQC (with a typical 0.2% or even lower fidelity), the complexity gap makes it almost impossible to generate meaningful reference data for the state-of-the-art quantum circuits. For example, for the comparison against Sycamore [11], the Summit supercomputer only manages to simulate a largely-simplified version with lower circuit depths up to 14, and the fidelity of the most complicated depth-20 case is projected based on the lower-depth simulations.

Several attempts have been made to narrow down the complexity gap set by Sycamore using the tensor network contraction (TNC) algorithm [21], powered by the recently developed excellent heuristic strategies to identify a near-optimal tensor network contraction order (TNCO) [22, 23]. Using a fused tensor contraction algorithm and a highly parallelized implementation on the new Sunway supercomputer, the runtime for computing a batch of correlated amplitudes for the depth-20 Sycamore RQC was reduced to about 300 seconds [24], which is currently further shortened to less than 150 seconds by using a lifetime theory to reduce the slicing overhead and increase the compute density [25]. For computing uncorrelated amplitudes, recently a dynamic global cache is adopted to reuse intermediate tensors and reduce the complexity, which computes millions of amplitudes for Sycamore RQCs up to depth 16 [26]. However validating the depth-20 case by exactly computing a large number of uncorrelated amplitudes is

* These authors contribute equally to this work.

† guochu604b@gmail.com

‡ lingan@tsinghua.edu.cn

§ haohuan@tsinghua.edu.cn

¶ lucyliu'zj@163.com

still out of reach. To this end we note that to attack the claim of quantum supremacy, several works have directly simulated the noisy RQC sampling by exploring biased noises to drastically reduce the computational cost [27, 28]. Here we focus on computing exact amplitudes instead, so as to provide a verification to noisy RQCs.

In this work, we manage to, for the first time, compute three million uncorrelated amplitudes of the most complicated depth-20 Sycamore RQC (referred to as Sycamore afterwards), using 107,520 SW26010P CPUs (41,932,800 cores) for 8.5 days. Built on both algorithmic and implementation-wise advances, we propose a multiple-amplitude TNC (ma-TNC) method whose performance greatly surpasses the previous works [22–25, 29] by at least three orders of magnitude. On the algorithmic side, we systematically explore the “classical advantage” of storing and reusing intermediate tensor results. We propose an improved loss function that searches for the optimal TNCO in terms of a minimized total complexity when reusing intermediate results among multiple amplitudes. We also provide a static caching strategy that identifies and stores the reusable results in such a way that minimizes both the compute cost and the memory overhead. On the implementation side, we build our simulator with a fused tensor network contraction algorithm to largely reduce data movement and increase compute density, and an adaptive parallelization scheme that fully utilizes the hundreds of cores in each processor for different sizes of tensors.

Our results provide a concrete verification for Sycamore, which is more than 10^3 times harder than simulating the noise sampling task itself. With further improvements for larger circuit sizes, we vision that the Zuchongzhi series of RQCs are also verifiable in the near term. Although we have focused on computing uncorrelated amplitudes of a RQC, our method is completely general for contracting a large number of similar tensor networks (TNs) which share a significant portion of common tensors. Therefore the ma-TNC algorithm and the parallelization techniques developed in this work could have a far-reaching impact beyond simulating RQCs, such as solving quantum many-body problems [30], statistics problems [31] or combinatorial optimization problems [32, 33].

II. MULTIPLE-AMPLITUDE SIMULATION WITH STATIC AND OPTIMAL TENSOR REUSE

For a quantum computer, due to the no-cloning theorem [34], the complexity of generating k samples from a RQC, denoted as \mathcal{S}_k , is strictly linear against k , namely

$$\mathcal{S}_k = k\mathcal{S} \quad (1)$$

where \mathcal{S} denotes the complexity of producing a single sample.

When simulating RQC on classical computers, the relation between \mathcal{S}_k and \mathcal{S} depends on the specific method we use. In the past three years, the method of choice to simulate Sycamore(-like) quantum processors has gradually converged to the TNC algorithm due to its relatively low computational complexity and well-controlled memory usage by using the slicing technique [22, 23]. The TNC algorithm transforms

the whole quantum circuit into a large TN (the original TN). Viewed in the time direction, this TN starts with n rank-1 tensors corresponding to the n input qubit states (often chosen as $|0\rangle$), which are followed by rank-2 and rank-4 tensors corresponding to the single-qubit and two-qubit gate operations (the size of each tensor index is 2). At the end of this TN there are n uncontracted tensor indices (output indices) which correspond to the output qubit states. Computing the amplitude of a given bitstring amounts to selecting the particular element of the uncontracted tensor indices according to this bitstring, resulting in a TN with no uncontracted indices. Computing k amplitudes will result in k different TNs, each with a specific choice of the output indices for the original TN.

In the following we present our ma-TNC algorithm for computing k amplitudes in detail. To proceed we first assume that we have already obtained a TNCO for computing one amplitude, which is shared for computing all the amplitudes. We will refer to those tensors in the original TN which contain at least one output index as the *bright tensors*. Following the TNCO, whenever a bright tensor is met, there could be a *branching*, which means that several TNs among all the k TNs share the same tensors till this bright tensor. Therefore, the computations before contracting this bright tensor can be perfectly reused among them. To systematically identify all such reusable patterns, we divide the original TN into many sub tensor networks (blocks) along the TNCO, where each block starts from a bright tensor and ends before the next bright tensor (the first block has no bright tensor), as shown in Fig. 1(a). Since there is a possible branching whenever a bright tensor is met, we organize the k TNs into a tree (the reuse tree) as shown in Fig. 1(b). Each node of the tree corresponds to one output index, while the edge after the node corresponds to a particular choice of this index. The nodes in the same vertical line correspond to the same output index and form a *layer*. A bright tensor containing multiple output indices would correspond to multiple layers. There could also exist tensors between successive bright tensors along the TNCO that do not contain any output indices, which are also assumed to live on the edges. Given these correspondences, a full path from left to right along the tree corresponds to contracting the TN for computing one amplitude, and traversing the tree corresponds to contracting all the k TNs. It is clear that all the intermediate computations before a certain node of the tree can be reused for the computations of all the subpaths after (and including) this node, thus an optimal reuse strategy would be to reuse all such computations to reduce the computational complexity.

We denote the computational complexity of one edge connecting a node in the l -th layer and another node in the $l+1$ -th layer as $\mathcal{S}_{l+1,l}$, then the complexity of one path is

$$\mathcal{S} = \sum_{l=0}^n \mathcal{S}_{l+1:l}. \quad (2)$$

Denoting the number of nodes in the l -th layer as w_l (the *width*), which is the same as the number of edges between the $(l-1)$ -th and l -th layers, then the computational complexity between the l -th layer and the $(l+1)$ -th layer is $w_{l+1}\mathcal{S}_{l+1:l}$

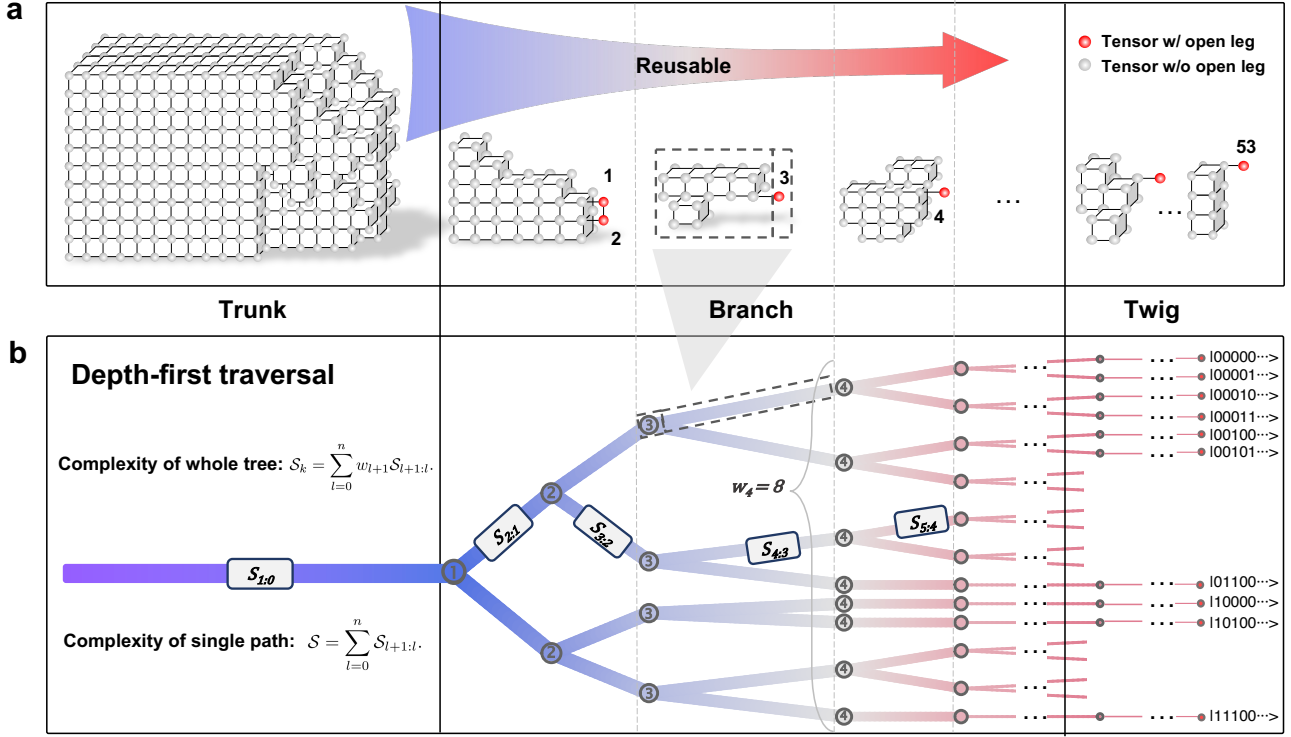


FIG. 1. **Demonstration of the ma-TNC algorithm.** (a) Division of the original tensor network formed in the TNC algorithm into consecutive sub tensor networks, where each sub tensor network starts with a bright tensor containing one or more output indices and ends before the next bright tensor. (b) Organizing the contraction of the k tensor networks resulting from computing k amplitudes into a tree, where each node of the tree corresponds to an output index and the edge after it corresponds to a specific choice of this index. A full path along the tree from left to right corresponds to contracting one tensor network and traversing the tree means to contract all the tensor networks. Generally for computing a large number of uncorrelated amplitudes, the left most edge (the trunk) contains most of the tensors, the number of edges in a vertical layer grows exponentially in the central part (the branch) and stops growing in the tail (the twig).

for optimal reuse, and the total complexity is

$$\mathcal{S}_k = \sum_{l=0}^n w_{l+1} \mathcal{S}_{l+1:l}. \quad (3)$$

w_l is non-decreasing with l which satisfies $w_1 = 1$, $w_{n+1} = k$ and $1 \leq w_l \leq k$ for $1 < l \leq n$. For computing a large number (but not exponentially large) of uncorrelated amplitudes, w_l will approximately grow exponentially at the beginning before it saturates. We will refer to the left most edge as the *trunk* since it usually contains most of the tensors in the original TN, the central part of the tree as the *branch* where most of the branching happen, and the tail as the *twig* where there is almost no branching.

From Eqs.(2, 3) we observe that $\mathcal{S}_k < k\mathcal{S}$ in general. A TNCO that minimizes \mathcal{S} does not necessarily minimize \mathcal{S}_k as well. Therefore to search for an optimal TNCO for computing k amplitudes, one should directly minimize Eq.(3) instead of Eq.(2). In fact, we observe that when using the optimal TNCO found by minimizing Eq.(3) to contract a single amplitude of Sycamore, the complexity is almost always higher than the optimal TNCO found by minimizing Eq.(2). However, the overall complexity of the former for computing three million amplitudes can be more than 10x lower than the latter.

To minimize the memory cost, one can perform a *depth-first traversal* of the tree, where one only needs to store all the intermediate tensors at the nodes in the branch along a single path from left to right. For Sycamore we found that the amount of memory required for a reuse-oriented computing of $3M$ amplitudes is only about two times that of computing a single amplitude. In comparison in the breath-first traversal one needs to store all the intermediate tensors at one layer, which could easily explode since the number of intermediate tensors to be stored scales with k . We summarize the defining features of our ma-TNC algorithm: 1) it directly minimizes the multi-amplitude complexity in Eq.(3) when searching for a near optimal TNCO and 2) it organizes the computation into a static tree and performs a depth-first traversal of the tree to accomplish the computation, which achieves optimal reuse of intermediate computations with minimal memory cost for a given TNCO. The static nature of our algorithm makes the tensor contraction pattern and the memory allocation predetermined, which is extremely important for massive parallelization.

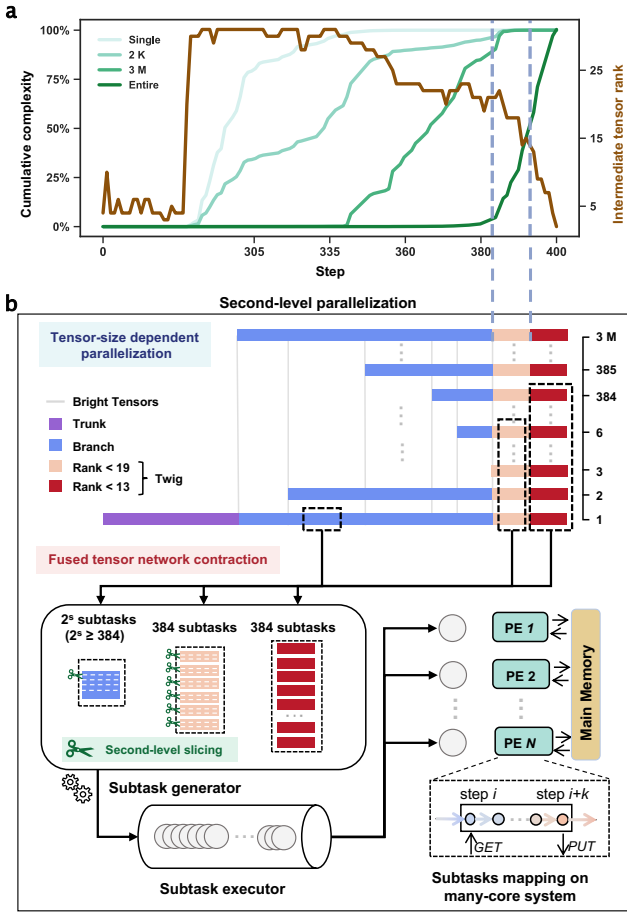


FIG. 2. Demonstration of the fused tensor network contraction and tensor-size dependent parallelization. (a) Distribution of the cumulative computational complexity (the blue lines to the left axis) and the intermediate tensor rank (the brown line to the right axis) along the tensor network contraction order. (b) Second-level parallelization on one SW26010P CPU for computing one slice (from the first-level slicing). In the trunk swTT is used for tensor contraction. In the branch and twig, the fused TNC algorithm is used which performs several tensor contractions locally on each core before fetching the result into the main memory. A tensor-size dependent parallelization scheme is also used to dynamically adjust the parallelization strategies for different tensor sizes such that the cores on a CPU can be fully utilized.

III. PARALLELIZING THE MA-TNC METHOD OVER 40 MILLION CORES OF THE NEW SUNWAY SUPERCOMPUTER

In our large-scale implementation on the new Sunway supercomputer, we use a two-level parallelization scheme. In the first level we use the slicing technique as a standard practice for the TNC algorithm to produce 2^{22} (≈ 4 million) slices for parallel processing [23, 24]. In the second level we contract each slice using our ma-TNC algorithm on each CPU.

Using our ma-TNC we can easily find a TNCO with $kS/S_k > 10^3$ for $k \approx 10^6$, which means that ideally we could achieve at least a 10^3 speedup compared to the single-

amplitude TNC (sa-TNC) algorithm where the amplitudes are computed independently. However, achieving such speedup poses great challenge in practice. In Fig. 2(a) we plot the distribution of computation along the different steps of TNCO. We can see that for the case of computing one amplitude, most computation falls into the region of large intermediate tensors (with tensor ranks ≈ 30). In contrast, for the case of computing millions of uncorrelated amplitudes, most computation concentrates in the branch where the tensors are much smaller (tensor ranks ≈ 20). The smaller sizes of the tensors involved in the ma-TNC algorithm result in a significant decrease of the compute density, and a lower computational efficiency, compared to the sa-TNC. Taking the case $k = 3M$ for example, we found a TNCO for which the ideal speedup compared to sa-TNC is 1328x, while the actual speedup using swTT (our previous tensor contraction implementation [24]) is only 40x. To restore the computational efficiency we propose a fused TNC algorithm, combined with an adaptive parallelization scheme that works differently with different tensor sizes. With these techniques we are able to restore the speedup of ma-TNC against sa-TNC from 40x to around 1248x. The algorithm is presented in the following based on the SW26010P CPU but the idea could be straightforwardly generalized to other heterogeneous architectures by adjusting the hyperparameters of the algorithm.

The central goal of the fused TNC algorithm is to perform several successive tensor contractions locally on each core before fetching the result tensor back into the main memory, thus the data movement between the main memory and the local memories (of the cores) can be largely reduced. The key for the performance of the fused TNC algorithm is to increase the number of tensor contractions that can be fused together, for which three techniques are used: 1) a proper rearrangement of the TNCO without complexity change to increase data overlap between successive tensor contractions; 2) a lifetime based second-level slicing of large tensors into smaller ones that fit into the local memories with no additional computational overhead; 3) exploring the sparsity of the reuse tree to fuse across the bright tensors without branching. In practice, the fused TNC algorithm is complemented with a tensor-size dependent parallelization scheme to fully utilize all the cores: for large tensors that would produce more slices than the cores to feed, we simply parallelize over the slices; for small tensors which can be directly stored on the local memory of a single core, we parallelize over different amplitudes; for medium-size tensors that are not able to produce enough slices, we parallelize over both the slices and the amplitudes. The fused TNC algorithm and the adaptive parallelization scheme are demonstrated in Fig. 2(b).

IV. SIMULATING SYCAMORE: PERFORMANCE AND RESULTS

We first evaluate the theoretical complexity and actual performance of our ma-TNC for simulating Sycamore, which is shown in Fig. 3. In Fig. 3(a) we show the scaling of the theoretical complexity of our ma-TNC against the number of

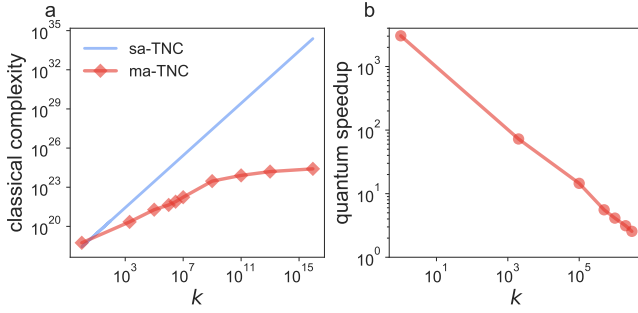


FIG. 3. **Theoretical complexity and actual performance of our ma-TNC.** (a) The red line with diamond shows the scaling of the theoretical complexity of our ma-TNC against the number of amplitudes k for Sycamore, while the blue line shows the linear scaling of the sa-TNC as a reference. (b) The quantum speedup of Sycamore against our ma-TNC, defined as our classical runtime divided by the quantum runtime, as a function of k .

amplitudes being computed, based on the optimal TNCO we found by minimizing Eq.(3). The scaling of the sa-TNC algorithm is shown as a reference. We can clearly see that the complexity of our ma-TNC scales sublinearly against k . For $k \approx 10^6$, ma-TNC already has a complexity which is lower than the sa-TNC by more than three orders of magnitude.

In Fig. 3(b) we show the actual performance of our ma-TNC using our well-optimized implementation on the new Sunway supercomputer, where we have also used the quantum runtime of Sycamore as the benchmarking baseline. The runtime for computing a single amplitude is assumed to be equivalent to that for generating a perfect sample using the TNC algorithm, since one could easily adjust the TNC algorithm to compute a small batch of correlated amplitudes with negligible overhead, and obtain a perfect sample with unit probability from the batch [23, 35]. Since we only compute exact amplitudes (perfect samples), the complexity of generating k perfect samples is assumed to be equivalent to that of generating k/f noisy samples with fidelity f [36]. The quantum speedup is then defined by the classical runtime of our ma-TNC on the new Sunway supercomputer divided by the quantum runtime of Sycamore. We can see that while the quantum speedup for generating one sample is more than 3,000x, it drastically decreases to 4x for generating 10^6 samples (and it will soon be slower than our ma-TNC if k further increases). Since quantum observables are inherently statistical and one generally needs to generate a large number of samples to maintain a certain level of confidence for the expectation values, the ability to speed up the calculation of multiple amplitudes will be useful for simulating any quantum algorithms in general besides the RQC sampling task.

Based on the algorithmic and implementation-wise advances, we are able to directly compute the exact amplitudes of three million experimentally generated samples by Sycamore, which is done by using 107,520 SW26010P CPUs for 8.5 days (203 hours). Our results show that the exact XEB fidelity for those three million bitstrings is $\mathcal{F}_{\text{XEB}} = (0.191 \pm 0.058)\%$, which closely matches the estimated value

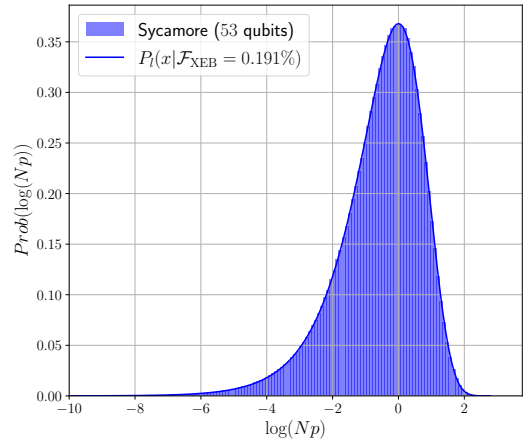


FIG. 4. **Verification of Sycamore.** Histogram for the distribution of the probabilities of the three million experimentally generated bitstrings from Sycamore, where the x-axis is log-rescaled. The blue solid line denotes the corresponding theoretical prediction under the same XEB fidelity as defined in Eq.(4).

of $(0.224 \pm 0.021)\%$ (We note that there are 10 groups of different RQCs with depth 20 and three million bitstrings are generated for each group in the original experiment [11], while we have only computed the amplitudes for one group due to limited computational resources). We plot in Fig. 4 the histogram of the obtained amplitudes and compare them to the theoretical probability density function for the rescaled bitstring probability Np ($N = 2^n$ and p is the probability) under the same XEB fidelity, defined as

$$P_l(x|\mathcal{F}_{\text{XEB}}) = (\mathcal{F}_{\text{XEB}}x + (1 - \mathcal{F}_{\text{XEB}})) e^{-x}, \quad (4)$$

with $x = Np$. We can see that they agree well with each other, which means that the bitstrings generated by Sycamore indeed obeys the Porter-Thomas distribution with the estimated XEB fidelity. Our results thus provide a strong consistency check for the Sycamore quantum supremacy experiment.

V. DISCUSSIONS

The Sycamore quantum processor performs a random circuit sampling task in which one million noise samples can be generated within 200 seconds. As a comparison we have computed three million amplitudes (whose complexity is the same as generating three million perfect samples) on the new Sunway supercomputer within 8.5 days, which is a task that is more than 10^3 harder than that performed by Sycamore. Taking into account that the complexity increases by the Zu-chongzhi series quantum processors are not dramatic compared to Sycamore (mostly due to that the increase is mostly in terms of the number of qubits instead of the gate fidelities [37]), we vision that those quantum processors can also be simulated in near term. Therefore although it is believed that the quantum processors will become exponentially more difficult to be simulated classically, our results indicate that we are again at a position that the most complicated quantum

circuits that can be implemented on current noisy quantum computers can be feasibly simulated and even verified using current classical supercomputers.

Other than simulating RQCs, our results also represent a major technical jump of the ability in contracting a large number of tensor networks with the same structure and sharing most of the tensors in common, which is a very universal situation that could be encountered in computational physics and combinatorial optimization problems and thus could be of very wide interest.

ACKNOWLEDGMENTS

The three million experimentally generated bitstrings are downloaded from <https://doi.org/10.1038/s41586-019-1666-5>. The bitstrings together with the calculated amplitudes are available at https://github.com/leao077/ma_TNC. We thank Xun Gao, Xiaobo Zhu, Zuoning Chen for helpful discussions and comments. This research was supported in part by the National Key Research and Development Plan of China (Grant No. 2020YFB0204800), National Natural Science Foundation of China (Grant No. T2125006, U1839206), Jiangsu Innovation Capacity Building Program (Project No. BM2022028). C. G acknowledges support from National Natural Science Foundation of China under Grants No. 11805279.

[1] R. P. Feynman, *International journal of theoretical physics* **21**, 467 (1982).

[2] P. Shor, in *Proceedings 35th Annual Symposium on Foundations of Computer Science* (1994) pp. 124–134.

[3] P. Krantz, M. Kjaergaard, F. Yan, T. P. Orlando, S. Gustavsson, and W. D. Oliver, *Applied Physics Reviews* **6**, 021318 (2019), <https://doi.org/10.1063/1.5089550>.

[4] H.-L. Huang, D. Wu, D. Fan, and X. Zhu, *Science China Information Sciences* **63**, 180501 (2020).

[5] S. Slussarenko and G. J. Pryde, *Applied Physics Reviews* **6**, 041303 (2019), <https://doi.org/10.1063/1.5115814>.

[6] R. Blatt and C. F. Roos, *Nature Physics* **8**, 277 (2012).

[7] C. D. Bruzewicz, J. Chiaverini, R. McConnell, and J. M. Sage, *Applied Physics Reviews* **6**, 021314 (2019), <https://doi.org/10.1063/1.5088164>.

[8] J. Biamonte, P. Wittek, N. Pancotti, P. Rebentrost, N. Wiebe, and S. Lloyd, *Nature* **549**, 195 (2017).

[9] S. McArdle, S. Endo, A. Aspuru-Guzik, S. C. Benjamin, and X. Yuan, *Rev. Mod. Phys.* **92**, 015003 (2020).

[10] J. Preskill, *Quantum* **2**, 79 (2018).

[11] F. Arute, K. Arya, R. Babbush, D. Bacon, J. C. Bardin, R. Barends, R. Biswas, S. Boixo, F. G. S. L. Brandao, D. A. Buell, B. Burkett, Y. Chen, Z. Chen, B. Chiaro, R. Collins, W. Courtney, A. Dunsworth, E. Farhi, B. Foxen, A. Fowler, C. Gidney, M. Giustina, R. Graff, K. Guerin, S. Habegger, M. P. Harrigan, M. J. Hartmann, A. Ho, M. Hoffmann, T. Huang, T. S. Humble, S. V. Isakov, E. Jeffrey, Z. Jiang, D. Kafri, K. Kechedzhi, J. Kelly, P. V. Klimov, S. Knysh, A. Korotkov, F. Kostritsa, D. Landhuis, M. Lindmark, E. Lucero, D. Lyakh, S. Mandrà, J. R. McClean, M. McEwen, A. Megrant, X. Mi, K. Michielsen, M. Mohseni, J. Mutus, O. Naaman, M. Neeley, C. Neill, M. Y. Niu, E. Ostby, A. Petukhov, J. C. Platt, C. Quintana, E. G. Rieffel, P. Roushan, N. C. Rubin, D. Sank, K. J. Satzinger, V. Smelyanskiy, K. J. Sung, M. D. Trevithick, A. Vainsencher, B. Villalonga, T. White, Z. J. Yao, P. Yeh, A. Zalcman, H. Neven, and J. M. Martinis, *Nature* **574**, 505 (2019).

[12] Y. Wu, W.-S. Bao, S. Cao, F. Chen, M.-C. Chen, X. Chen, T.-H. Chung, H. Deng, Y. Du, D. Fan, M. Gong, C. Guo, C. Guo, S. Guo, L. Han, L. Hong, H.-L. Huang, Y.-H. Huo, L. Li, N. Li, S. Li, H. Rong, H. Su, L. Sun, L. Wang, S. Wang, D. Wu, Y. Xu, K. Yan, W. Yang, Y. Yang, Y. Ye, J. Yin, C. Ying, J. Yu, C. Zha, C. Zhang, H. Zhang, K. Zhang, Y. Zhang, H. Zhao, Y. Zhao, L. Zhou, C.-Y. Lu, C.-Z. Peng, X. Zhu, and J.-W. Pan, *Phys. Rev. Lett.* **127**, 180501 (2021).

[13] Q. Zhu, S. Cao, F. Chen, M.-C. Chen, X. Chen, T.-H. Chung, H. Deng, Y. Du, D. Fan, M. Gong, C. Guo, C. Guo, S. Guo, L. Han, L. Hong, H.-L. Huang, Y.-H. Huo, L. Li, N. Li, S. Li, Y. Li, F. Liang, C. Lin, J. Lin, H. Qian, D. Qiao, H. Rong, H. Su, L. Sun, L. Wang, S. Wang, D. Wu, Y. Wu, Y. Xu, K. Yan, W. Yang, Y. Yang, Y. Ye, J. Yin, C. Ying, J. Yu, C. Zha, C. Zhang, H. Zhang, K. Zhang, Y. Zhang, H. Zhao, Y. Zhao, L. Zhou, C.-Y. Lu, C.-Z. Peng, X. Zhu, and J.-W. Pan, *Science Bulletin* **67**, 240 (2022).

[14] M. J. Bremner, A. Montanaro, and D. J. Shepherd, *Phys. Rev. Lett.* **117**, 080501 (2016).

[15] S. Boixo, S. V. Isakov, V. N. Smelyanskiy, R. Babbush, N. Ding, Z. Jiang, M. J. Bremner, J. M. Martinis, and H. Neven, *Nature Physics* **14**, 595 (2018).

[16] A. Bouland, B. Fefferman, C. Nirkhe, and U. Vazirani, *Nature Physics* **15**, 159 (2019).

[17] D. Hangleiter and J. Eisert, [arXiv:2206.04079](https://arxiv.org/abs/2206.04079) (2022).

[18] S. Aaronson and L. Chen, in *Proceedings of the 32nd Computational Complexity Conference, CCC '17* (Schloss Dagstuhl–Leibniz-Zentrum fuer Informatik, Dagstuhl, DEU, 2017).

[19] S. Aaronson and S. Gunn, *Theory of Computing* **16**, 1 (2020).

[20] D. Aharonov, X. Gao, Z. Landau, Y. Liu, and U. Vazirani, [arXiv:2211.03999](https://arxiv.org/abs/2211.03999) (2022).

[21] I. L. Markov and Y. Shi, *SIAM Journal on Computing* **38**, 963 (2008), <https://doi.org/10.1137/050644756>.

[22] J. Gray and S. Kourtis, *Quantum* **5**, 410 (2021).

[23] C. Huang, F. Zhang, M. Newman, X. Ni, D. Ding, J. Cai, X. Gao, T. Wang, F. Wu, G. Zhang, H.-S. Ku, Z. Tian, J. Wu, H. Xu, H. Yu, B. Yuan, M. Szegedy, Y. Shi, H.-H. Zhao, C. Deng, and J. Chen, *Nature Computational Science* **1**, 578 (2021).

[24] Y. A. Liu, X. L. Liu, F. N. Li, H. Fu, Y. Yang, J. Song, P. Zhao, Z. Wang, D. Peng, H. Chen, C. Guo, H. Huang, W. Wu, and D. Chen, in *Proceedings of the International Conference for High Performance Computing, Networking, Storage and Analysis*, SC '21 (Association for Computing Machinery, New York, NY, USA, 2021).

[25] Y. Chen, Y. Liu, X. Shi, J. Song, X. Liu, L. Gan, C. Guo, H. Fu, D. Chen, and G. Yang, [arXiv:2205.00393](https://arxiv.org/abs/2205.00393) (2022).

[26] G. Kalachev, P. Panteleev, and M.-H. Yung, [arXiv:2108.05665](https://arxiv.org/abs/2108.05665)

(2021).

[27] F. Pan, K. Chen, and P. Zhang, *Phys. Rev. Lett.* **129**, 090502 (2022).

[28] X. Gao, M. Kalinowski, C.-N. Chou, M. D. Lukin, B. Barak, and S. Choi, *arXiv:2112.01657* (2021), <https://arxiv.org/abs/2112.01657>.

[29] F. Pan and P. Zhang, *Phys. Rev. Lett.* **128**, 030501 (2022).

[30] R. Orús, *Nature Reviews Physics* **1**, 538 (2019).

[31] M. Mézard, G. Parisi, and M. A. Virasoro, *Spin glass theory and beyond: An Introduction to the Replica Method and Its Applications*, Vol. 9 (World Scientific Publishing Company, 1987).

[32] M. Mézard, G. Parisi, and R. Zecchina, *Science* **297**, 812 (2002), <https://www.science.org/doi/pdf/10.1126/science.1073287>.

[33] M. Mezard and A. Montanari, *Information, physics, and computation* (Oxford University Press, 2009).

[34] W. K. Wootters and W. H. Zurek, *Nature* **299**, 802 (1982).

[35] B. Villalonga, S. Boixo, B. Nelson, C. Henze, E. Rieffel, R. Biswas, and S. Mandrà, *npj Quantum Information* **5**, 86 (2019).

[36] I. L. Markov, A. Fatima, S. V. Isakov, and S. Boixo, *arXiv:1807.10749* (2018).

[37] A. Zlokapa, S. Boixo, and D. Lidar, *arXiv:2005.02464* (2020), <https://arxiv.org/abs/2005.02464>.